Experimental Safety Assessment of Degraded EV Battery Modules: Insights from High-Current Testing and Thermal Behavior

Michał Łanocha and Maksymilian Mądziel *

Posted Date: 7 April 2026

doi: 10.20944/preprints202604.0461.v1

Keywords: battery degradation; cell voltage imbalance; high-current discharge; SOH assessment; thermal runaway precursors; EV safety

 doi:10.20944/preprints202604.0461.v1

Article

Experimental Safety Assessment of Degraded EV Battery Modules: Insights from High-Current Testing and Thermal Behavior

Michał Łanocha [1] and Maksymilian Mądziel [1,*]

Faculty of Mechanical Engineering and Aeronautics, Rzeszow University of Technology, 35-959 Rzeszow, Poland

* Correspondence: mmadziel@prz.edu.pl

Featured Application

The experimental safety assessment methodology presented here is directly applicable to EV fleet operators, automotive workshops, and battery recycling facilities handling aging Nissan Leaf 30 kWh packs. It provides a practical diagnostic workflow—from LeafSpy OBD screening to high-current bench testing with infrared monitoring—for identifying and isolating critically imbalanced modules (>200 mV delta under load) before thermal runaway risks emerge. The approach enables cost-effective module replacement strategies, extending vehicle service life while mitigating safety hazards during high-power transients (acceleration, hill climbing) in real-world operation.

Abstract

This study presents an experimental safety assessment of degraded lithium-ion battery modules from a 2016 Nissan Leaf 30 kWh pack (106,394 km) exhibiting P33E6 faults, "turtle mode" activation, and sudden range drops. On-vehicle diagnostics using LeafSpy revealed severe cell voltage imbalance, with a 2323 mV spread across 96 cells under high-current load (165–170 A), individual cells dropping to 1.041 V. Laboratory capacity testing of modules 73–88 (16S2P configuration) measured 49.8 Ah (4.1–3.1 V) versus nominal 84 Ah, confirming SOH 59% (vs. BMS-reported 57%). High-current discharge (600 W → 40 A) of the weakest segment (cells 81–84) demonstrated critical safety limits: cell 82 voltage collapsed from 4.04 V to 1.2 V within 56 minutes, cell voltage delta escalated from 20 mV to 810 mV after 38 minutes, culminating in open-circuit failure. Infrared thermography recorded localized surface heating to 43 °C (ΔT = 24 K above 19 °C ambient) with irreversible cell swelling, indicating early thermal runaway precursors. The findings validate LeafSpy OBD diagnostics for identifying at-risk modules and underscore the necessity of high-power bench testing with thermal monitoring for aging EV packs. Fleet operators should prioritize module replacement for cells showing >200 mV load delta to prevent sudden power loss and thermal events in 30 kWh Nissan Leaf vehicles.

Keywords: battery degradation; cell voltage imbalance; high-current discharge; SOH assessment; thermal runaway precursors; EV safety

1. Introduction

The ongoing electrification of road transport is increasingly shaped by ambitious climate and industrial policies [1,2]. In the European Union, the Fit for 55 framework has set a clear long-term direction toward zero-emission new cars and vans from 2035, while parallel policy measures in other markets, including the United Kingdom and several non-European jurisdictions, are accelerating the deployment of electric vehicles and charging infrastructure [3,4]. This regulatory momentum is not only transforming vehicle markets and supply chains, but also increasing the importance of battery

 doi:10.20944/preprints202604.0461.v1

durability, in-service diagnostics, and end-of-life safety, especially as the first large wave of early-generation EVs enters the phase of extended real-world aging [5,6].

The rapid expansion of electric vehicle (EV) adoption has led to increasing attention on the long-term reliability, degradation mechanisms, and safety of lithium-ion battery systems [7,8]. Early-generation EVs, such as the Nissan Leaf 30 kWh (2016–2017), represent an important case study due to their widespread deployment and long-term exposure to real-world aging effects. After extended operation (typically 8–10 years and over 100,000 km), these battery systems frequently exhibit accelerated degradation phenomena, including capacity fade, increased internal resistance, and significant cell voltage imbalance.

A large body of literature has investigated lithium-ion battery aging, with a focus on fundamental degradation mechanisms such as solid electrolyte interphase (SEI) growth, lithium plating, and loss of active material [9,10]. These processes are strongly coupled and lead to loss of lithium inventory (LLI), impedance increase, and overall reduction of battery performance [11,12]. Comprehensive reviews confirm that degradation is inherently multi-physical, involving electrochemical, thermal, and mechanical phenomena that evolve over time [13,14].

In particular, batteries based on nickel–manganese–cobalt (NMC) and lithium–manganese oxide (LMO) chemistries—commonly used in early Nissan Leaf models—are known to suffer from both calendar aging and cycling-induced degradation, especially under elevated temperatures and high state-of-charge conditions [15]. Experimental studies on commercial NMC cells have demonstrated that aging leads to resistance growth, gas generation, electrode expansion, and electrolyte decomposition, all of which contribute to performance loss and potential failure [16].

While capacity fade mechanisms are relatively well understood, fewer studies have addressed the safety implications of operating degraded battery packs under high-power transient conditions, such as rapid acceleration or hill climbing [17,18]. Under such conditions, internal resistance differences between cells result in uneven current distribution and significant voltage imbalance. Voltage differences exceeding 200–500 mV across cells is widely recognized as indicative of abnormal operation and advanced degradation.

Several studies have shown that degraded cells with elevated internal resistance experience disproportionate voltage drops under load, which may force individual cells below safe operating limits. This behavior is directly linked to increased heat generation, accelerated degradation, and risk of internal failure mechanisms such as lithium plating or internal short circuits [19,20]. Moreover, degradation-induced phenomena such as electrolyte decomposition, gas evolution, and mechanical deformation (e.g., swelling) are well-documented precursors to thermal instability [21,22].

The vulnerability of EV battery packs is further exacerbated by module-level architecture. In configurations with parallel cell groups, such as the 4S2P layout used in the Nissan Leaf, weaker cells disproportionately affect current distribution, accelerating imbalance growth and increasing the likelihood of localized failure. These effects are amplified during high-current transients (150–200 A), where voltage sag becomes highly non-uniform across the pack.

In parallel with laboratory-based studies, recent research emphasizes the importance of diagnostic and monitoring techniques for early detection of degradation. Electrochemical impedance spectroscopy (EIS), post-mortem analysis, and data-driven methods are commonly used to identify degradation modes and assess state-of-health (SOH) [23,24]. However, the relationship between in-vehicle diagnostics and actual safety limits under high-load conditions remains insufficiently explored.

This study addresses this gap by combining on-vehicle diagnostics with controlled laboratory testing of degraded battery modules from a real-world Nissan Leaf vehicle (106,394 km, 58 quick-charge sessions). Using OBD-based diagnostics, the full 96-cell voltage distribution was analyzed under both high- and low-current conditions, enabling the identification of critically imbalanced modules (cells 73–88). These modules were subsequently extracted and subjected to laboratory testing, including capacity evaluation (16S2P configuration, 4.1–3.1 V) and high-current discharge experiments (600 W → 40 A) with infrared thermal monitoring.

 doi:10.20944/preprints202604.0461.v1

The main contributions of this work can be summarized as follows:

- Experimental validation of the correlation between OBD-detected cell imbalance and laboratory-measured SOH (59% vs. 57% BMS-reported),
- Time-resolved analysis of cell voltage divergence leading to failure (20 mV → 810 mV),
- Identification of thermal and mechanical failure precursors (43 °C surface temperature, cell swelling) under high-current conditions,
- Demonstration of safety risks associated with operating degraded EV battery modules during high-power transients.

Despite extensive research on lithium-ion battery degradation and state-of-health estimation, several important gaps remain in the context of real-world EV operation. First, most existing studies focus either on controlled laboratory aging experiments or on simulation-based analyses, while relatively few works investigate batteries that have undergone long-term real-world usage under combined calendar and cycling stress conditions. Second, although cell voltage imbalance is widely recognized as a key indicator of degradation, its direct relationship with extreme voltage collapse under high-current transients (down to ~1 V per cell) has not been sufficiently quantified in the literature. Third, there is a lack of integrated methodologies linking non-invasive in-vehicle diagnostics (e.g., OBD-based monitoring) with destructive laboratory testing to validate safety limits and failure mechanisms.

Therefore, there is a clear need for experimental studies that bridge the gap between non-invasive field diagnostics and controlled high-current laboratory testing, providing quantitative insight into the safety risks of operating severely degraded EV battery modules under realistic load conditions. These findings offer practical insights for fleet operators, automotive workshops, and battery recycling facilities, contributing to improved diagnostic strategies, safer operation of aging EV battery systems, and a comprehensive framework for assessing the safety of second-life battery applications.

2. Materials and Methods

The analyzed vehicle was a 2016-model Nissan Leaf (Figure 1) equipped with a 30 kWh lithium-ion battery pack, rated at a nominal voltage of 400 V DC and a nominal capacity of 83 Ah. The traction motor was rated at 80 kW (109 hp) with a maximum torque of 254 Nm. As-found mileage at the time of testing was 106 394 km, corresponding to a relatively high real-world usage intensity for an early-generation LEAF.

Figure 1. The vehicle under test and a photo of the removed battery pack.

The battery pack consists of multiple 4S2P modules, where each module is formed by four series-connected cells and two parallel strings, resulting in a higher total voltage while maintaining sufficient current-handling capability. The pack is monitored and controlled by an OEM Nissan BMS,

 doi:10.20944/preprints202604.0461.v1

which reports the State-of-Health (SOH) and various voltage and temperature parameters both in-vehicle and via the on-board diagnostics (OBD) interface.

The scheme of the work is presented in Figure 2. The study follows a structured experimental workflow for assessing the safety of degraded lithium-ion battery modules from an electric vehicle. The process begins with vehicle selection and on-board diagnostics using the LeafSpy application connected via OBD interface. Key operational parameters, including state of charge (SOC), pack voltage, current, temperature, and individual cell voltages, are recorded under both high- and low-load conditions.

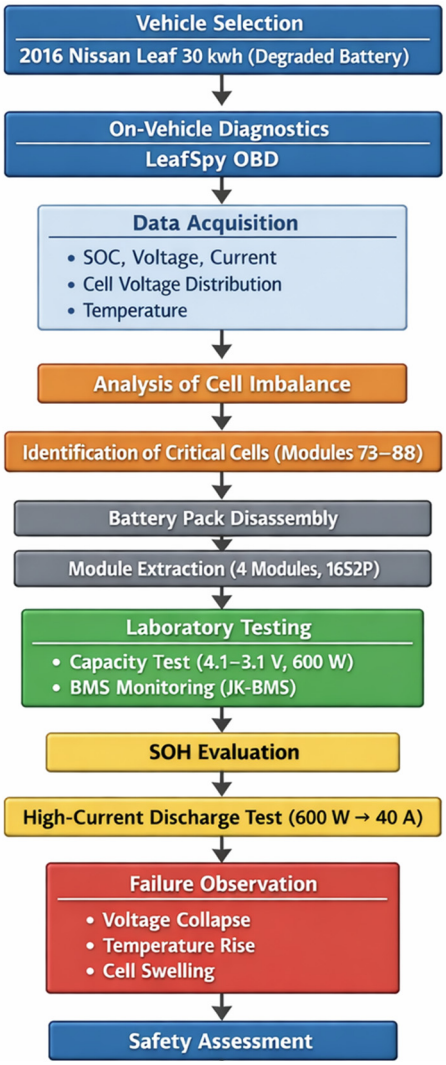

Figure 2. Workflow of the experimental methodology for safety assessment of degraded EV battery modules.

Based on the collected data, cell voltage imbalance analysis is performed to identify the most degraded segments of the battery pack. Modules exhibiting the highest voltage deviation (cells 73–88) are selected for further investigation. The battery pack is then safely disassembled, and the selected modules are extracted for laboratory testing.

In the laboratory phase, the modules are reconfigured into a 16S2P setup and subjected to controlled capacity testing within the 4.1–3.1 V range using a 600 W load, while being monitored by an external BMS system. The measured capacity is used to evaluate the state of health (SOH) and compare it with the BMS-reported value.

Subsequently, the weakest cell segment (cells 81–84) is selected for high-current discharge testing to assess safety limits under extreme operating conditions. During this test, time-resolved

 doi:10.20944/preprints202604.0461.v1

measurements of individual cell voltages, voltage differences, and thermal behavior are recorded, including infrared thermography.

The experiment concludes with the observation of failure mechanisms such as voltage collapse, rapid increase in cell voltage imbalance, temperature rise, and physical deformation (swelling). These results form the basis for safety assessment and practical recommendations regarding early detection and replacement of degraded battery modules.

2.1. On-Vehicle Diagnostics and Fault Description

The primary objective of the on-vehicle tests was to diagnose the root cause of a sudden drop in the indicated driving range and periodic loss of power, accompanied by the activation of the so-called "turtle mode", where the vehicle speed is limited to about 40 km/h. The vehicle owner reported that under hard acceleration the propulsion system briefly loses power and triggers a "traction system fault" warning, after which continued driving is only possible in service mode with significantly reduced motor power. The Nissan BMS recorded error code P33E6, which is associated with cell-voltage-imbalance or low-voltage conditions in the high-voltage battery pack. To quantify the state-of-charge (SOC), high-voltage (HV) pack voltage, current and temperature, the vehicle was monitored using the LeafSpy application connected via an OBDII adapter. Typical logged parameters included SOC (≈66–74%), HV pack voltage (around 350 V at the time of the test), HV current up to about 170 A under heavy load, and several temperature readings across the pack. The BMS-reported SOC stability and range display were found to be highly erratic under dynamic driving conditions, with displayed range values dropping from about 150 km to ca. 30 km during aggressive acceleration events.

2.2. Test Setup and Data Acquisition

For on-vehicle diagnostics, an OBDII-to-Bluetooth interface (ELM327-based) was used to connect the Nissan Leaf BMS to a smartphone running LeafSpy. The software recorded real-time data from the high-voltage traction battery, including cell-voltage distribution, pack current, pack voltage, SOC, pack temperature, and 12-V auxiliary battery parameters. Cellular-level data were recorded at a few seconds' interval, enabling a snapshot of the pack state under both quiescent and high-load conditions.

Measurements were taken under two main conditions:

- High-current condition: full-throttle acceleration starting from ca. 67% SOC, held for about 6 s at maximum available current (≈165–170 A), while recording the transient voltage drop and cell-voltage spread.
- Low-current condition: low-load, steady-state driving at around 40% SOC, where the pack current was typically below 30 A, to capture the baseline cell-voltage distribution.

All raw data were exported from LeafSpy and post-processed using Python (Matplotlib, Pandas) to generate cell-voltage bar plots and statistical summaries (min/avg/max cell voltage, cell-voltage delta, temperature spread). The same data set was used to infer the overall pack degradation and to identify the segments of cells with the most critical voltage deviation.

2.3. Module Selection, Disassembly and Safety Precautions

The highest-impact cells identified from the OBDII data were those numbered 73–88, which exhibited the largest voltage deviations and lowest voltages during high-current operation. These cells were located within four 4S2P battery modules that were therefore selected for further laboratory testing. The battery pack cover was safely removed in accordance with the manufacturer's guidelines and workshop safety protocols for high-voltage systems.

Prior to module removal, the high-voltage traction system was deactivated, the pack was discharged to a safe SOC level, and the service-mode procedure was applied to isolate the traction battery. The four selected modules were then carefully disconnected from the pack and isolated using

 doi:10.20944/preprints202604.0461.v1

appropriate personal protective equipment (PPE) and high-voltage safety tools. Each module was cleaned and visually inspected for any visible damage, swelling or leakage before being connected to the test bench.

2.4. Capacity Test of Degraded Modules

Each of the four selected modules was individually equipped with a custom mechanical compression fixture to ensure the same level of compression as the original battery pack, thereby maintaining proper cell-to-cell contact and avoiding mechanical stress increase during thermal expansion. The four modules were interconnected in series to form a 16S2P assembly (16 cells in series, 2 parallel strings), which corresponds to the same cell configuration as in the original pack segment.

A third-party JK-BMS 150 A (8–16S) was used to monitor and protect the test assembly. The BMS was configured to the appropriate cell count (16S) and calibrated with known reference voltages. The pack was first charged at constant current until the voltage per cell reached 4.1 V – a level at which the Nissan Leaf BMS assumes 100% SOC, remaining below the typical 4.2 V limit used in many consumer Li-ion applications.

Following the charge phase, the test pack was discharged using a 600 W battery tester operating in constant-power mode until the cell voltage dropped to 3.1 V – a level at which the original Nissan Leaf BMS assumes 0% SOC, and which is close to its lower cut-off voltage. The total coulombic capacity delivered during the 4.1–3.1 V discharge was recorded as 49.8 Ah.

During the test, the BMS-built-in capacity estimator, cycle counter and remaining-capacity display were also recorded, along with the average cell voltage (≈3.52 V) and cell-voltage difference (≈58 mV) to quantify the remaining in-pack imbalance. Temperature sensors on the BMS board (MOS temperature and two battery temperature channels) were used to ensure the pack stayed within a safe thermal envelope (ca. 23–25 °C ambient-like conditions).

2.5. High-Current Discharge Safety Test

In addition to the quasi-static capacity test, a high-current discharge test was performed on a single weak segment (cells 81–84) to assess its safety margins under extreme load. This segment was selected based on the on-vehicle OBDII data, where cell 82 consistently exhibited the lowest voltage and the largest voltage drop under high-current conditions, indicating elevated internal resistance and/or advanced degradation.

The test was conducted without the BMS protection, using only a 600 W/40 A battery tester and a manual digital multimeter for voltage and current monitoring. The segment was initially charged to a resting voltage of about 4.04–4.05 V per cell. The test began at t = 0 min, with the tester operating in constant-power mode (600 W). When the pack voltage dropped below about 15 V, the tester automatically switched to constant-current mode (40 A) to maintain the load.

Voltage measurements for each cell (81–84) were manually recorded at predefined time intervals (0, 2, 4, 28, 33, 38, 43, 46, 51, 56 min). The cell-voltage delta was computed as the difference between the maximum and minimum cell voltages within the segment at each time step. The test was terminated at 56 min upon clear signs of cell failure:

- Electrical: one cell opened the circuit (the multimeter showed OL when the probes were placed directly on the poles). After waiting, the multimeter measured 1.2 V across that series.
- Thermal: an infrared camera recorded a local temperature of 43 °C on the exterior of the failing cell, while the ambient temperature was ca. 19 °C. The cell visibly swelled and did not return to its original shape after cooling for several hours.

All high-current tests were performed inside a ventilated enclosure with appropriate fire-safety equipment and thermal monitoring to ensure safe observation of the early-stage thermal-runaway-like behavior. The collected time-series data were used to plot the individual cell voltages and the evolving cell-voltage delta, serving as a basis for the safety assessment in the Results section.

 doi:10.20944/preprints202604.0461.v1

3. Results

Figure 3 presents the cell-voltage distribution of the 30 kWh Nissan Leaf battery pack as recorded via LeafSpy under high-current load (165.66 A) at a SOC of 74.2%. The pack shows a total cell-voltage delta of 2.323 V (2323 mV) across the 96 cells, indicating significant imbalance during the full-acceleration event. Key metrics include Ahr=45.16, SOH=58.82%, Hx=25.13%, and pack voltage around 288–290 V (inferred from average cell levels near 3 V).

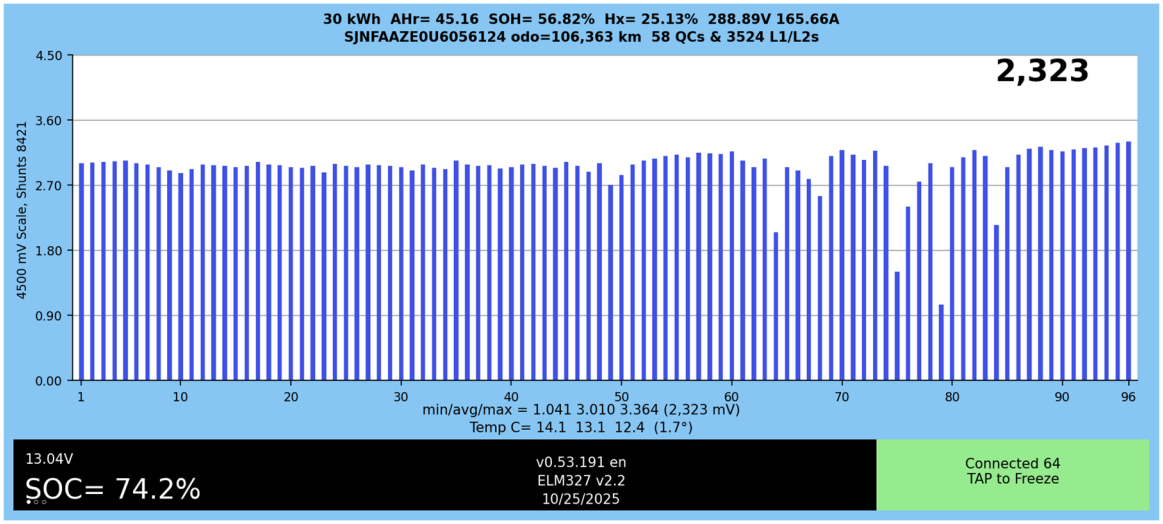

Figure 3. The cell-voltage distribution under high-current conditions.

A snapshot, presented in Figure 4, shows the cell-voltage distribution under low-current conditions (SOC ≈ 40%, pack current ≈ 25–30 A). Here the cell-voltage spread is markedly reduced but still non-negligible, with a minimum cell voltage of about 3.554 V, an average of 3.631 V, and a maximum of 3.721 V (delta ≈ 167 mV). The pack voltage was around 348 V under these conditions, confirming that the pack still retains a relatively high nominal voltage level despite advanced degradation. The 12-V auxiliary battery voltage remained stable at about 13.04 V, indicating that the power-management system and low-voltage components are not directly responsible for the traction-system faults.

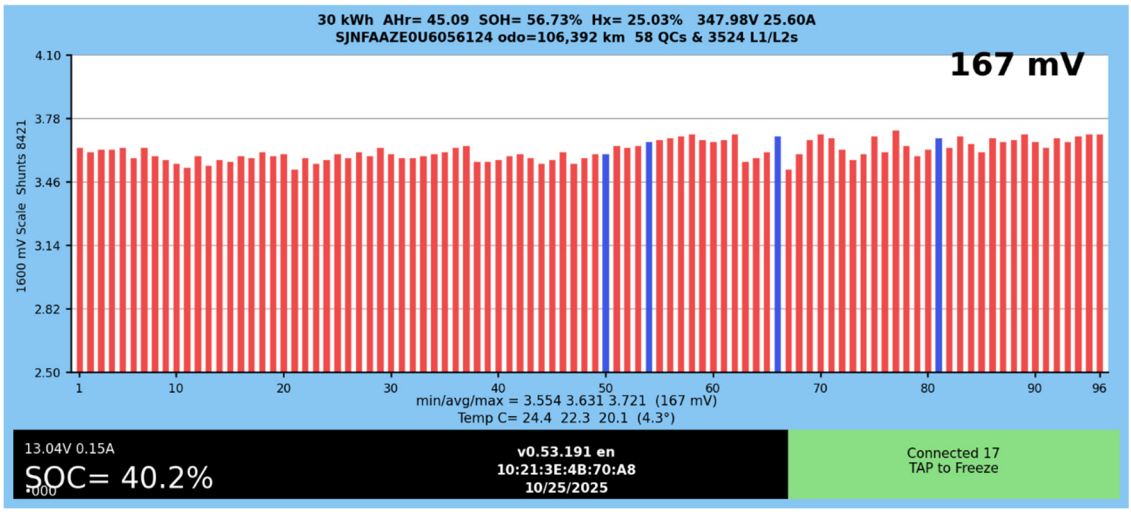

Figure 4. The cell-voltage distribution under low-current conditions.

These results confirm earlier observations in the literature that cell-voltage spreads in the tens of millivolts can be considered acceptable in healthy LEAF packs, while triple-digit millivolt deviations under load are indicative of severe cell-imbalance or advanced degradation. The observed

 doi:10.20944/preprints202604.0461.v1

spread in the tested pack is consistent with reported symptoms of "turtle mode" activation and range-indicator instability, as the on-board BMS likely limits power once the lowest-voltage cell approaches the cut-off threshold.

3.1. Capacity Test and SOH Assessment of Degraded Modules

Table 1 presents the BMS-reported parameters recorded during the capacity test of the four selected modules (cells 73–88, configured as 16S2P). The average cell voltage was 3.516 V, with a maximum cell-voltage difference of 58 mV, indicating a moderate remaining imbalance within the segment. The pack voltage was 56.26 V at the start of the test, and the pack current was −10.8 A during the constant-power (600 W) discharge phase. The BMS-estimated capacity of the segment was 66.0 Ah, with 23.2 Ah remaining at the end of the test (≈35% of the BMS capacity).

Table 2 summarizes the statystyki napięć i rezystancji ogniw from the same test. The measured capacity obtained from the external 600 W battery tester, integrated over the 4.1–3.1 V discharge window, was 49.8 Ah. Given the nominal module capacity of 84 Ah for the 30 kWh Nissan Leaf pack, the laboratory-determined SOH is:

$$SOH_{lab} = \frac{49.8}{84} \approx 59\% \quad (1)$$

This value is slightly higher than the on-board BMS-reported SOH of ca. 57%, consistent with studies showing BMS-derived SOH can be conservative. Cell-wire resistances were mostly in the range of 0.038–0.059 Ω, supporting moderate internal resistance growth.

Table 1. BMS-reported parameters during capacity test (16S2P, cells 73–88).

Parameter	Value
Charge	ON
Discharge	ON
Balance	OFF
Main Voltage	56.26 V
Main Current	−10.8 A
Battery Power	607.3 W
Battery Capacity	66.0 Ah
Remain Capacity	23.2 Ah
Remain Battery	35%
Cycle Count	1
Cycle Capacity	88.8 Ah
Time Emerg.	0
Time Enter Sleep	86400 s
LCD Buzzer Alarm	OFF
Ave. Cell Volt.	3.516 V
Cell Volt. Diff.	0.058 V
Balance Curr.	0.000 A
MOS Temp.	23.6 °C
Battery T1	23.6 °C
Battery T2	25.4 °C
Detail Logs Count	129
Cell Type	Li-ion
Measured Capacity Tester (4.1–3.1 V)	49.8 Ah

Table 2. Voltage statistics for the tested cells (N = 16).

Metric	Min	Mean	Max	Delta
Voltage_V	3.479	3.516	3.538	0.059

 doi:10.20944/preprints202604.0461.v1

The cell voltages recorded during the test showed a maximum spread of 59 mV, with the minimum individual cell voltage at 3.479 V and the maximum at 3.538 V. This moderate imbalance is consistent with the on-vehicle observations and indicates progressive cell degradation, though no immediate critical voltage deviation was present under the test conditions.

3.2. High-Current Discharge of the Weakest Segment (Cells 81–84)

Figure 5 shows the individual cell voltages of the weakest segment (cells 81–84) during a 56-minute high-current discharge test at 600 W (switching to 40 A when the pack voltage dropped below about 15 V). At the beginning of the test (t = 0 min), all four cells were at resting voltages around 4.04–4.05 V, corresponding to a high SOC level within the 4.1–3.1 V window.

The most notable behavior is observed after about 38 min of continuous discharge, when the cell-voltage spread suddenly increases and cell 82 begins to deviate significantly from the others. By 43 min, the cell-voltage delta reaches about 810 mV, with cell 82 dropping to 2.25 V while the other cells remain above 3 V. This situation persisted until the 56th minute of the test, when the voltage measurement showed 1.2 V on that cell, indicating a near-catastrophic internal failure or short-circuit. (The multimeter displayed OL when the probes were placed directly on the poles, and after a waiting period measured approximately 1.2 V.)

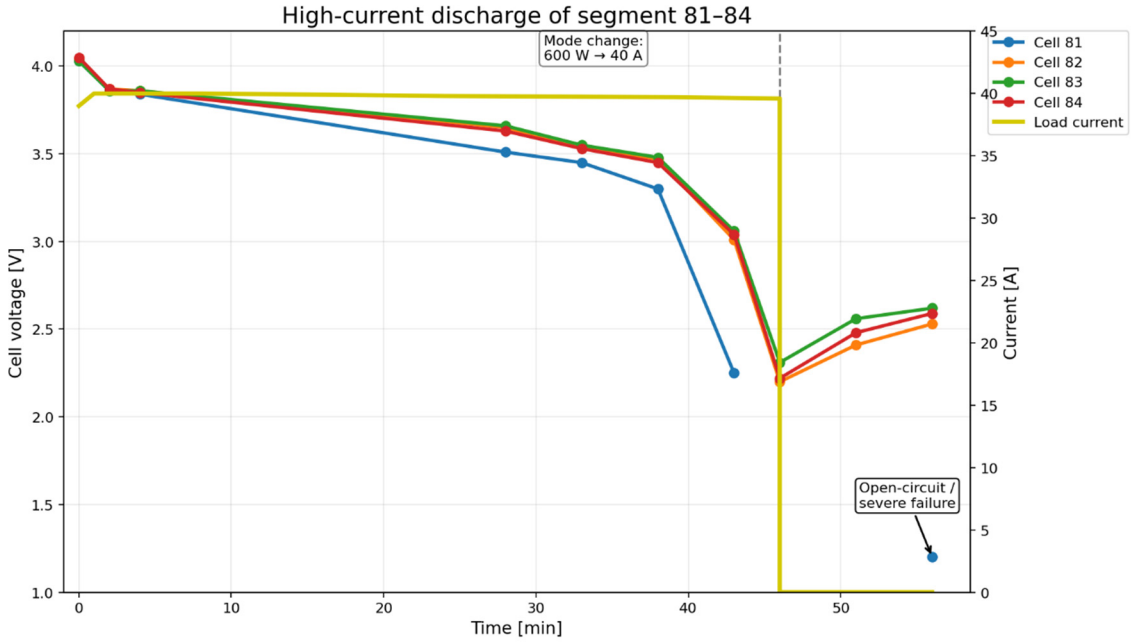

Figure 5. The individual cell voltages of the weakest segment (cells 81–84).

Figure 6 presents the cell-voltage delta (maximum minus minimum cell voltage within the segment) over time. The delta remains relatively low during the first 30 minutes (typically below 100–150 mV), but then rises sharply after 38 min, reaching 810 mV at 43 min and exceeding 1.5 V by the end of the test. This rapid increase in voltage spread is a known precursor to unsafe operation in lithium-ion battery packs, as the weakest cell is forced to carry a disproportionate share of the voltage drop and generates excess heat.

 doi:10.20944/preprints202604.0461.v1

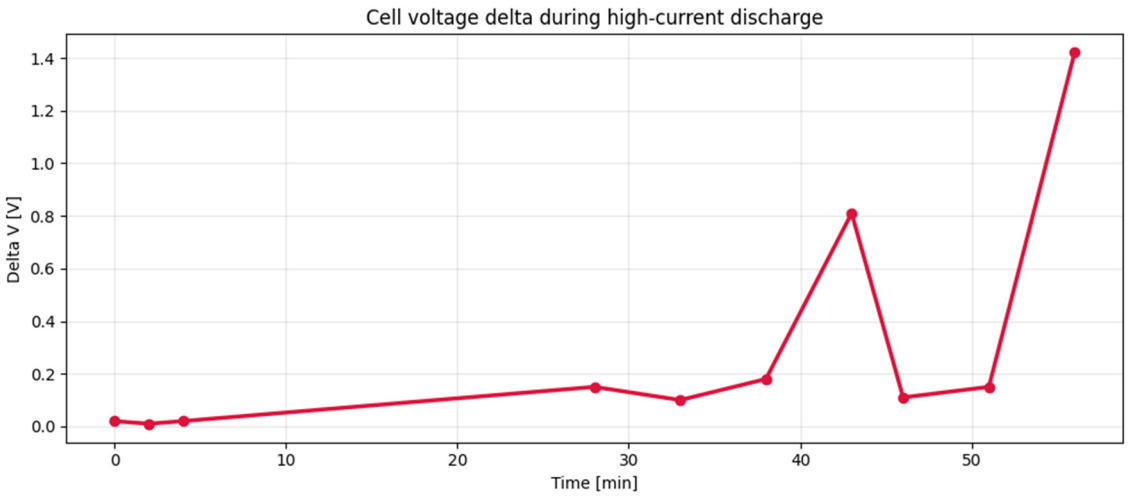

Figure 6. The cell-voltage delta (maximum minus minimum cell voltage within the segment) over time.

3.3. Thermal Behavior and Safety Implications

Thermal measurements using an infrared camera (Figure 7) show that the surface temperature of the failing cell (cell 82) reached about 43 °C at the moment of failure, while the ambient temperature was ca. 19 °C. This corresponds to a temperature rise of about 24 K above ambient, which is consistent with experimental studies showing that high-current discharge rates can increase cell surface temperature to similar levels even without full-scale thermal runaway.

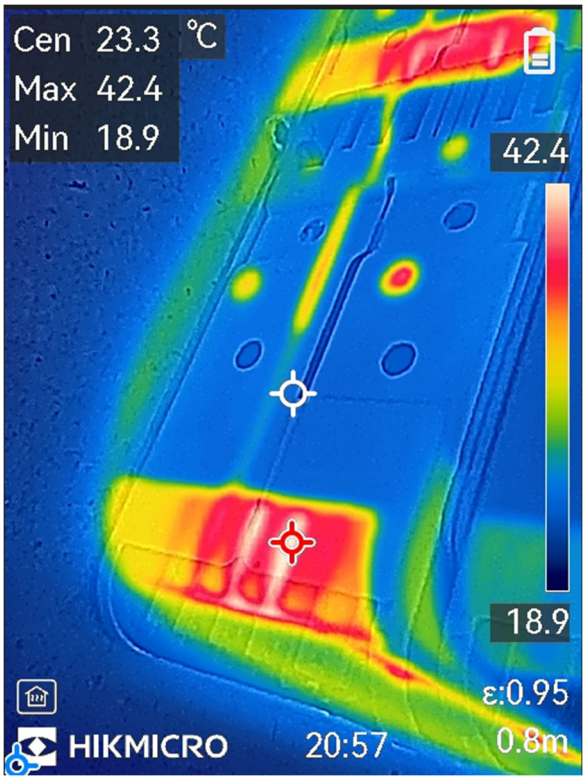

Figure 7. Thermal measurements using an infrared camera.

Visually, the cell exhibited pronounced swelling and did not return to its original shape after cooling for several hours, indicating irreversible mechanical damage and electrolyte decomposition. The temperature of the module as a whole approached ambient condition only after about 3 h, suggesting that the thermal-inertia effects are significant in such densely packed modules. These

 doi:10.20944/preprints202604.0461.v1

observations are consistent with early-stage thermal-runaway behavior in lithium-ion cells, where localized heating and swelling precede full-scale venting or fire.

4. Discussion

The experimental results clearly demonstrate that the observed P33E6 fault code, “turtle mode” activation, and sudden range drops in the analyzed 2016 Nissan Leaf are strongly correlated with severe cell voltage imbalance under high-current conditions. The measured voltage spread of 2323 mV across 96 cells during a short 6-second acceleration event (165–170 A) significantly exceeds values typically reported for aged lithium-ion packs, where imbalance under load is usually limited to several hundred millivolts [25]. Such an extreme deviation confirms that the weakest cells are driven far beyond their safe operating limits, explaining both the activation of BMS protection mechanisms and the observed loss of propulsion performance.

The observed voltage imbalance of 2323 mV is significantly higher than values typically reported in the literature for aged lithium-ion battery packs. For example, studies on commercial EV cells indicate that voltage spreads under high-load conditions usually remain within the range of 100–500 mV, even for moderately degraded systems [25]. The magnitude observed in this study therefore represents an extreme case of cell divergence, indicating near-failure conditions at the pack level.

The laboratory capacity test results further validate the reliability of on-board diagnostics. The close agreement between the measured SOH (59%) and the BMS-reported value (57%) is consistent with previous studies showing that modern BMS algorithms provide relatively accurate but slightly conservative estimates of battery health [26]. Similar discrepancies (2–5%) have been reported in experimental studies comparing field data with laboratory measurements, where BMS systems intentionally underestimate capacity to ensure operational safety margins [27]. The observed 58 mV cell voltage spread during controlled discharge confirms that, under moderate load conditions, the modules still operate within a quasi-stable regime, despite advanced degradation. The measured voltage collapse to approximately 1.2 V is particularly noteworthy, as most experimental studies report cut-off voltages in the range of 2.5–3.0 V under standard operating conditions [25]. Values approaching 1 V are rarely documented in the literature and are typically associated with severe internal degradation or imminent cell failure, including internal short-circuit formation or lithium depletion.

However, the high-current discharge test of the weakest segment (cells 81–84) reveals critical safety implications that are not captured by standard capacity measurements. The rapid increase in voltage imbalance—from 20 mV to 810 mV within a relatively short time frame—demonstrates the nonlinear nature of degradation under load. Similar behavior has been reported in studies on aged lithium-ion cells, where internal resistance growth leads to accelerated divergence of cell voltages under high-current conditions [28]. The observed voltage collapse of cell 82 (from 4.04 V to 1.2 V) indicates a near-complete loss of electrochemical functionality, likely associated with internal short-circuit formation or severe lithium depletion.

The thermal response recorded during the experiment provides further insight into the failure mechanisms. The measured surface temperature of 43 °C (ΔT = 24 K above ambient) is consistent with early-stage thermal instability reported in the literature, where localized heating precedes full thermal runaway events [29]. Importantly, the absence of immediate thermal runaway despite clear electrical failure aligns with findings that degraded cells may undergo prolonged pre-failure phases characterized by gradual heat accumulation, gas evolution, and mechanical deformation [30]. The observed cell swelling confirms irreversible structural damage, which is commonly linked to electrolyte decomposition and gas generation. The recorded temperature increase (ΔT = 24 K) is consistent with reported thermal responses of lithium-ion cells under high discharge rates, where temperature rises of 10–30 K are commonly observed prior to thermal runaway initiation [29]. However, in contrast to studies reporting rapid transition to thermal runaway at higher temperatures (>80 °C), the present results indicate that significant electrical failure and mechanical degradation

 doi:10.20944/preprints202604.0461.v1

may occur at relatively moderate temperatures (~40–45 °C), highlighting the importance of early-stage detection.

Compared to existing studies, the key contribution of this work lies in the direct linkage between field diagnostics and destructive laboratory testing. While previous research has either focused on controlled laboratory aging [31] or on in-vehicle monitoring data [32], relatively few studies have combined both approaches in a single experimental framework. This integration enables a more realistic assessment of safety risks, as it captures both operational conditions and failure mechanisms under controlled stress scenarios.

Furthermore, the results highlight the limitations of pack-level monitoring strategies. As demonstrated, pack voltage and SOC values remained within acceptable ranges even when individual cells experienced critical failure. This observation supports previous findings that cell-level heterogeneity is a major challenge in battery management, particularly in aged packs with parallel configurations [33]. The 4S2P architecture used in the Nissan Leaf exacerbates this issue, as degraded cells impose additional stress on parallel counterparts, accelerating imbalance growth and increasing failure probability.

This observation is consistent with findings in second-life battery studies, where cells with SOH levels in the range of 60–80% may still exhibit unsafe behavior under dynamic loading conditions [34]. This confirms that capacity-based metrics alone are insufficient for assessing operational safety in aged battery systems.

From a practical perspective, the findings confirm that voltage imbalance under load is a more reliable safety indicator than static capacity metrics. While a SOH of approximately 60% may still be considered acceptable for daily operation, the results clearly show that high-power transients expose hidden safety risks. Similar conclusions have been reported in studies on second-life battery applications, where cells with moderate capacity loss may still exhibit unsafe behavior under dynamic loading conditions [35].

The implications for fleet operators and maintenance practices are significant. The results suggest that OBD-based diagnostic tools, such as LeafSpy, can effectively identify at-risk modules prior to catastrophic failure, provided that measurements are performed under sufficiently high load conditions. Moreover, the use of high-current bench testing combined with thermal monitoring offers a valuable method for validating safety margins and identifying failure-prone cells before reuse or repurposing.

Overall, the tested 30 kWh Nissan Leaf battery pack demonstrates that while nominal degradation to SOH ≈ 60% remains functionally acceptable, the underlying electrochemical heterogeneity introduces critical safety limitations. These limitations become evident only under high-current conditions, highlighting the need for more advanced diagnostic approaches that account for dynamic operating scenarios rather than relying solely on static performance indicators.

Despite the valuable insights provided, this study has several limitations that should be considered when interpreting the results.

First, the analysis is based on a single vehicle and battery pack, which limits the generalizability of the findings across different EV models, usage patterns, and battery chemistries. While the observed degradation behavior is consistent with known mechanisms, further studies on a larger sample size are required to confirm the universality of the results. Second, the high-current discharge test was performed on a selected weak segment rather than the entire battery pack. Although this approach allows for detailed observation of failure mechanisms, it does not fully capture pack-level interactions during extreme operating conditions. Third, the experimental setup did not include advanced diagnostic techniques such as electrochemical impedance spectroscopy (EIS) or post-mortem material analysis, which could provide deeper insight into the underlying degradation processes at the electrode level. Finally, the study focuses on short-term high-current behavior and does not address long-term thermal propagation or full thermal runaway scenarios. Future research should investigate the progression from early-stage failure to full-scale thermal events under controlled conditions.

 doi:10.20944/preprints202604.0461.v1

5. Conclusions

This study provides a comprehensive experimental assessment of the safety limits of degraded lithium-ion battery modules from a real-world 2016 Nissan Leaf 30 kWh battery pack. The results demonstrate that severe cell voltage imbalance is the primary driver of observed operational issues, including P33E6 fault activation, "turtle mode" limitation, and sudden range collapse.

The combination of on-board diagnostics and laboratory testing confirms that, although the battery retains a moderate state-of-health (SOH ≈ 59%), its internal heterogeneity leads to critical safety risks under high-current conditions. In particular, the observed voltage collapse of an individual cell from 4.04 V to 1.2 V, accompanied by a rapid increase in voltage imbalance (up to 810 mV) and localized temperature rise (ΔT = 24 K), demonstrates that failure mechanisms can develop well before complete pack-level degradation.

From a practical perspective, the results highlight that voltage imbalance under load is a more reliable indicator of safety risk than conventional capacity-based metrics. The study also confirms that OBD-based diagnostic tools, such as LeafSpy, can effectively identify at-risk modules when combined with high-load testing conditions.

The proposed methodology—integrating field diagnostics with controlled high-current testing and thermal monitoring—provides a practical framework for early detection of failure-prone cells in aging EV battery systems. This approach is particularly relevant for fleet management, maintenance strategies, and second-life battery applications, where safety considerations are critical.

Future work should focus on expanding the dataset to multiple vehicles and battery chemistries, as well as developing predictive models linking voltage imbalance dynamics with failure probability under real-world operating conditions.

Author Contributions: Conceptualization, M.Ł. and M.M.; methodology, M.Ł.; software, M.Ł.; validation, M.M.; formal analysis, M.M.; investigation, M.Ł.; resources, M.Ł.; data curation, M.Ł. writing—original draft preparation, M.Ł.; writing—review and editing, M.M.; visualization, M.Ł.; supervision, M.M; project administration, M.M.; funding acquisition, M.M. All authors have read and agreed to the published version of the manuscript.

Funding: This research received no external funding.

Data Availability Statement: The original contributions presented in this study are included in the article. Further inquiries can be directed to the corresponding author.

Conflicts of Interest: The authors declare no conflicts of interest.

Abbreviations

The following abbreviations are used in this manuscript:

DT	Digital Twin
ITS	Intelligent Transport Systems
IoT	Internet of Things
AIM	Adaptive Inflow Metering
SiL	Software-in-the-Loop
LOS	Level of Service
GEH	Geoffrey E. Havers (statistic used in traffic modelling)
TMC	Traffic Management Center
SUMP	Sustainable Urban Mobility Plan
ZTM	Zarząd Transportu Miejskiego (Municipal Transport Authority)
COM	Component Object Model (interface)
PM	Particulate Matter
NOx	Nitrogen Oxides
QLEN	Queue Length
STOPDELAY	Stop Delay per Vehicle

 doi:10.20944/preprints202604.0461.v1

References

1. Koroma, M. S., & Alwosheel, A. (2026). Aligning vehicle electrification with power sector transitions: life cycle insights across diverse grids. npj Sustainable Mobility and Transport, 3(1), 9.
2. Mądziel, M.; Kulasa, P.; Campisi, T. Determinants of Test-to-Reality CO**2** *Gaps in European PHEVs: The Limited Role of Battery Capacity. Vehicles 2026*, *8*, **60.** https://doi.org/10.3390/vehicles8030060
3. Guven, D., Kayalica, M. O., & Bozdag, C. E. (2026). Assessing policy interventions for electric vehicle adoption through an agent-based environmental framework. Applied Energy, 407, 127338.
4. Mądziel, M. State of Charge Prediction for Li-Ion Batteries in EVs for Traffic Microsimulation. Energies 2025, 18, 4992. https://doi.org/10.3390/en18184992
5. Tokito, S., & Nakamoto, Y. (2025). Differences in vehicle electrification policies and optimal transition periods across countries. Journal of Industrial Ecology, 29(3), 878-890.
6. Mądziel, M.; Campisi, T. Predictive Artificial Intelligence Models for Energy Efficiency in Hybrid and Electric Vehicles: Analysis for Enna, Sicily. *Energies* 2024, *17*, 4913. https://doi.org/10.3390/en17194913
7. Rufino Júnior, C. A., Sanseverino, E. R., Gallo, P., Amaral, M. M., Koch, D., Kotak, Y., ... & Zanin, H. (2024). Unraveling the degradation mechanisms of lithium-ion batteries. Energies, 17(14), 3372.
8. Mądziel, M.; Campisi, T. Predicting Auxiliary Energy Demand in Electric Vehicles Using Physics-Based and Machine Learning Models. Energies 2025, 18, 6092. https://doi.org/10.3390/en18236092
9. Li, R., Kirkaldy, N. D., Oehler, F. F., Marinescu, M., Offer, G. J., & O'Kane, S. E. (2025). The importance of degradation mode analysis in parameterising lifetime prediction models of lithium-ion battery degradation. Nature communications, 16(1), 2776.
10. Tong, L., Li, Y., Xu, Y., Fang, J., Wen, C., Zheng, Y., ... & Gong, M. (2025). A combined method for state-of-charge estimation for lithium-ion batteries based on IGWO-ASRCKF and ELM under various aging levels. Journal of Energy Storage, 124, 116843.
11. Seo, G., Ha, J., Kim, M., Park, J., Lee, J., Park, E., ... & Lee, J. (2022). Rapid determination of lithium-ion battery degradation: High C-rate LAM and calculated limiting LLI. Journal of Energy Chemistry, 67, 663-671.
12. Peng, Y., Zhong, C., Ding, M., Zhang, H., Jin, Y., Hu, Y., ... & Yang, Y. (2024). Quantitative analysis of active lithium loss and degradation mechanism in temperature accelerated aging process of lithium-ion batteries. Advanced Functional Materials, 34(42), 2404495.
13. Arif, N. A., Mekhilef, S., Seyedmahmoudian, M., & Stojcevski, A. (2026). Degradation in Li-ion batteries and capacity decline under different cycling conditions: A comprehensive review. Journal of Energy Storage, 154, 121270.
14. Schreiber, M., Gamra, K. A., Bilfinger, P., Teichert, O., Schneider, J., Kröger, T., ... & Lienkamp, M. (2025). Understanding lithium-ion battery degradation in vehicle applications: Insights from realistic and accelerated aging tests using Volkswagen ID. 3 pouch cells. Journal of Energy Storage, 112, 115357.
15. Madani, S. S., Shabeer, Y., Allard, F., Fowler, M., Ziebert, C., Wang, Z., ... & Khalilpour, K. (2025). A comprehensive review on lithium-ion battery lifetime prediction and aging mechanism analysis. Batteries, 11(4), 127.
16. Gasper, P., Sunderlin, N., Dunlap, N., Walker, P., Finegan, D. P., Smith, K., & Thakkar, F. (2024). Lithium loss, resistance growth, electrode expansion, gas evolution, and Li plating: Analyzing performance and failure of commercial large-format NMC-Gr lithium-ion pouch cells. Journal of Power Sources, 604, 234494.
17. Mądziel, M. Impact of Weather Conditions on Energy Consumption Modeling for Electric Vehicles. *Energies 2025, 18, 1994.* https://doi.org/10.3390/en18081994
18. Naiek, S. M., Aungsuthar, S., Harper, C., & Hendrickson, C. (2025). Battery electric vehicle safety issues and policy: a review. World Electric Vehicle Journal, 16(7), 365.
19. Bai, P., Li, J., Brushett, F. R., & Bazant, M. Z. (2016). Transition of lithium growth mechanisms in liquid electrolytes. Energy & Environmental Science, 9(10), 3221-3229.
20. Rehnlund, D., Wang, Z., & Nyholm, L. (2022). Lithium-diffusion induced capacity losses in lithium-based batteries. Advanced Materials, 34(19), 2108827.

 doi:10.20944/preprints202604.0461.v1

21. Sharifi-Asl, S., Lu, J., Amine, K., & Shahbazian-Yassar, R. (2019). Oxygen release degradation in Li-ion battery cathode materials: mechanisms and mitigating approaches. Advanced Energy Materials, 9(22), 1900551.
22. Cabana, J., Kwon, B. J., & Hu, L. (2018). Mechanisms of degradation and strategies for the stabilization of cathode–electrolyte interfaces in Li-ion batteries. Accounts of chemical research, 51(2), 299-308.
23. Mauger, A., & Julien, C. M. (2017). Critical review on lithium-ion batteries: are they safe? Sustainable?. Ionics, 23(8), 1933-1947.
24. Sun, J. Y., Wang, Z. Y., Shen, X., Wu, Y., & Cheng, X. B. (2026). Thermal Runaway Mechanisms and Mitigation Strategies of Silicon-Based Anode in Lithium-Ion Batteries: A Review. Advanced Energy Materials, 16(9), e05793.
25. Dubarry, M., Qin, N., & Brooker, P. (2018). Calendar aging of commercial Li-ion cells of different chemistries–A review. Current Opinion in Electrochemistry, 9, 106-113.
26. Berecibar, M., Gandiaga, I., Villarreal, I., Omar, N., Van Mierlo, J., & Van den Bossche, P. (2016). Critical review of state of health estimation methods of Li-ion batteries for real applications. Renewable and Sustainable Energy Reviews, 56, 572-587.
27. Farmann, A., & Sauer, D. U. (2016). A comprehensive review of on-board State-of-Available-Power prediction techniques for lithium-ion batteries in electric vehicles. Journal of Power Sources, 329, 123-137.
28. Keil, P. (2017). Aging of lithium-ion batteries in electric vehicles (Doctoral dissertation, Technische Universität München).
29. Feng, X., Zheng, S., Ren, D., He, X., Wang, L., Cui, H., ... & Ouyang, M. (2019). Investigating the thermal runaway mechanisms of lithium-ion batteries based on thermal analysis database. Applied Energy, 246, 53-64.
30. Spotnitz, R., & Franklin, J. (2003). Abuse behavior of high-power, lithium-ion cells. Journal of power sources, 113(1), 81-100..
31. Keil, P., & Jossen, A. (2017). Temperature-Dependent Aging of Lithium-Ion Batteries Analyzed by Differential Voltage Analysis. In AABC Europe 2017.
32. Schuster, S. F., Bach, T., Fleder, E., Müller, J., Brand, M., Sextl, G., & Jossen, A. (2015). Nonlinear aging characteristics of lithium-ion cells under different operational conditions. Journal of Energy Storage, 1, 44-53.
33. Barré, A., Deguilhem, B., Grolleau, S., Gérard, M., Suard, F., & Riu, D. (2013). A review on lithium-ion battery ageing mechanisms and estimations for automotive applications. Journal of power sources, 241, 680-689.
34. Iqbal, H., Sarwar, S., Kirli, D., Shek, J. K., & Kiprakis, A. E. (2023). A survey of second-life batteries based on techno-economic perspective and applications-based analysis. *Carbon Neutrality*, *2*(1), 8.
35. Li, J., He, S., Yang, Q., Wei, Z., Li, Y., & He, H. (2022). A comprehensive review of second life batteries toward sustainable mechanisms: Potential, challenges, and future prospects. IEEE Transactions on Transportation Electrification, 9(4), 4824-4845.